Research Article

iMedPub Journals
http://www.imedpub.com

Insights in Analytical Electrochemistry
ISSN 2470-9867

2018
Vol.4 No.1:1

DOI: 10.21767/2470-9867.100023

# Sulfolan with $LiPF_6$, $LiNTf_2$ and LiBOB - as a Non-Flammable Electrolyte Working in a Cell with a $LiNiO_2$ Cathode

**Beata Kurc***

Institute of Chemistry and Electrochemistry, Faculty of Chemical Technology, Poznan University of Technology, Berdychowo 4, PL-60965 Poznan, Poland

## Abstract

$LiNiO_2$ was examined as cathode materials for the lithium-ion battery, working with non-flammable electrolyte, obtained by dissolution of solid lithium bis(trifluoromethanesulphonyl)imide ($LiNTf_2$), lithium bis(oxalato)borate (LiBOB) and lithium hexa fluorophosphate ($LiPF_6$, Fluka) in sulfolane (TMS) with 10% vinylene carbonate (VC). The Li/$LiNiO_2$ cells were tested by cyclic voltammetry, galvanostatic charging/discharging. The $LiNiO_2$ cathode showed good cyclability and coulombic efficiency for the electrolyte, which contains 1 M $LiPF_6$ in TMS+10%VC (195 and 140 $mAhg^{-1}$ after 20 cycles-C/10). Correspondingly lower capacity was observed for system Li/$LiNiO_2$ in: 1 M $LiNTf_2$ in TMS+10%VC and 1 M LiBOB in TMS+10%VC. The $LiNiO_2$ (solid)+1 M $LiPF_6$+TMS+10%VC system show a flash point of ca. 160°C (classical $LiNiO_2$+1 M $LiPF_6$+EC 50%+DMC 50% system: $T_f \approx 42$°C).

**Keywords:** Sulfolane; Li-ion battery; Cathodes; $LiNiO_2$; Impedance spectra

**Received:** January 30, 2018; **Accepted:** February 08, 2018; **Published:** February 15, 2018

**Corresponding author:** Beata Kurc

beata.kurc@put.poznan.pl

Institute of Chemistry and Electrochemistry, Faculty of Chemical Technology, Poznan University of Technology, Berdychowo 4, PL-60965 Poznan, Poland.

**Tel:** +48616652571

**Citation:** Kurc B (2018) Sulfolan with $LiPF_6$, $LiNTf_2$ and LiBOB - as a Non-Flammable Electrolyte Working in a Cell with a $LiNiO_2$ Cathode. Insights Anal Electrochem Vol.4 No.1:1

## Introduction

Lithium ion batteries (LIBs) have become the most prominent choice of power source for all types of portable microelectronic devices, as they offer higher energy density than the other rechargeable power sources [1,2]. Development of a highly efficient, thin film positive electrode which can provide high cell voltage, high specific capacity and cycling stability even at rapid charge/discharge rates, is the key issue of electrochemical research [3,4]. Good Enough et al. was the first to report a layered lithium cobalt oxide ($LiCoO_2$) positive electrode material in the 1980's. In the practice major limitation is connected with the removal of Li from $LixCoO_2$ i.e., de lithiation of $LiCoO_2$ restricted to x Ľ 0.5, which corresponds to 4.2 V vs. Li/Li (a capacity value of 140 $mAhg^{-1}$). However, several efforts have been expended to extract extra capacity and to cycle the $LiCoO_2$ cathode beyond 4.2 V so as to increase energy density of the LIB's [2-17]. This would be connected with obtain: desirable properties of $LiCoO_2$ as a cathode without post deposition heat treatments at elevated temperatures [7,9], replacing a part of base transition metal (Co) with another element (Ni, Mn, Ti, Fe etc.) [10,11], surface modification of $LiCoO_2$ films with inert metal oxides (MOx, M Ľ Al, Mg, Sn, Zn, Zr) and inorganic salts ($AlF_3$, $Al(OH)_3$, $AlPO_4$) [12] and development of various nano-structured $LiCoO_2$ materials [13-16] and tailoring the morphological properties [17,18].

$LiNiO_2$ is known to be difficult to synthesize and its multi-phase reactions during electrochemical cycling lead to structural degradation [19-30]. During the charge process, $LiNiO_2$ undergoes a sequential change in its crystal structure from the hexagonal phase to the monoclinic phase, to the hexagonal phase again, followed by two hexagonal phases, and finally a single hexagonal phase [31]. There are also concerns over the thermal stability of $LiNiO_2$ in the charged state. To overcome the difficulties with its synthesis and structural instability during cycling and to improve thermal safety, the nickel ion has been substituted by various metal ions (e.g., Mg, Al, Mn, Ga) [32-35]. It has been reported that the substitution process stabilizes the crystal structure of the material during the intercalation/deintercalation of lithium ions, even in an overcharged state, and there by improves $LiNiO_2$ cycle ability. A molten-salt method has been found to be a simple means to prepare pure and stoichiometric powders of multi-component oxides, in which the molten salts are utilized as solvent or reacting species [36,37]. Since the diffusion rates of the components in molten salts are much higher than those in a solid-state reaction, various powders, such as $LiCoO_2$, can

 

be prepared at significantly lower temperatures [38]. Han et al. [38,39] investigated the preparation of $LiCoO_2$ and $LiCo_{0.8}M_{0.2}O_2$ (M=Al, Ni) by molten-salt synthesis.

The general aim of this study was to investigate a new electrolyte: 1 M $LiPF_6$ in TMS+10%VC; 1 M $LiNTf_2$ in TMS+10%VC and 1 M LiBOB in TMS+10%VC working in both systems Li/$LiCoO_2$ and Li/$LiNiO_2$.

# Experimental

## Materials

Graphite, (G, SL-20, BET surface area 6.0 $m^2g^{-1}$, Superior Graphite, USA), carbon black, (CB, Fluka), poly(vinylidene fluoride) (PVdF, Fluka), sulfolane (TMS, Fluka), lithium foil (Aldrich, 0.75 mm thick), vinylene carbonate (VC, Aldrich), *N*-methyl-2-pyrrolidinone (NMP, Fluka), lithium bis(trifluoro methane sulfonyl)imide ($LiNTf_2$, Fluka), lithium hexa fluorophosphate ($LiPF_6$, Fluka), lithium bis(oxalato)borate (LiBOB Fluka), $LiNiO_2$ powder (Aldrich) were used as purchased. Electrolytes were obtained by dissolution of the solid $LiPF_6$, $LiNTf_2$ and LiBOB salts in liquid TMS heated to ca. 35°C (TMS is solid at room temperature). Electrolytes contained VC as a SEI forming additive (10%). Tested $LiNiO_2$ and $LiCoO_2$ cathodes were prepared by casting $LiNiO_2$/$LiCoO_2$+G+ PVdF (ratio 85:5:10) slurry in N-methyl-2-pyrrolidinone (NMP, Fluka) on the current collector (diameter 12 mm) (NMP was evaporated in vacuum at 120°C).

## Apparatus and measurements

Particle size distributions were determined for $LiNiO_2$. Measurements were performed on a Zeta sizer Nano ZS made by Malvern Instruments Ltd. UK, using the non-invasive back scattering method (NIBS). From the particle size distribution the polydispersity index was calculated, which provides information on the homogeneity of the product particles. The morphology and microstructure of the products were examined using a scanning electron microscope (Zeiss EVO40). From these images it was also possible to determine the particle structures and their tendency towards aggregation or agglomeration.

The performances of the cells were characterized using galvanostatic charge-discharge tests. Cycling efficiency of $LiNiO_2$|Li, $LiNiO_2$|G systems was measured in two compartment cells. Electrodes were separated by the glass microfiber GF/A separator (Whatmann), placed in an adopted 0.5 Swagelok® connecting tube. Typically, the mass of electrodes was as follows: Li: ca. 45 mg (0.785 $cm^2$) and cathode: 2.0-3.0 mg, graphite: 3.0-4.0 mg. The cells were assembled in a glove box in the dry argon atmosphere. The cycling measurements were taken with the use of the ATLAS 0461 MBI multichannel electrochemical system (Atlas-Sollich, Poland) at different current rates (C/10-C/2). Cyclic voltammetry (CV) and ac impedance measurements were performed using the µAutolab FRA2 type III electrochemical system (Ecochemie, Netherlands).

Thermal gravimetric analysis was conducted with the use of the STA 449 F3 Jupiter TG/DTA analyser (NETZSCH-Gerätebau GmbH) with the 2°C $min^{-1}$ rate. Flash point of the electrolyte was measured with an open cup home-made apparatus, based on the Cleveland open cup instrument, with a 1.5 ml cup. The cup was heated electrically through a sand bath, and temperature was measured with the M-3850 (Metex, Korea) digital thermometer. The apparatus was scaled with a number of compounds of known flash points.

# Results

## PSD and morphology

**Figure 1** shows particle size distributions and SEM images of $LiNiO_2$ (a, b) and $LiCoO_2$ (c, d) respectively. $LiNiO_2$ is characterised

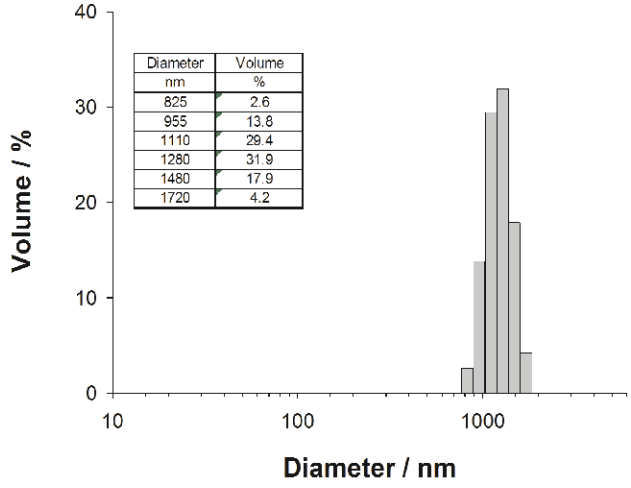


a)

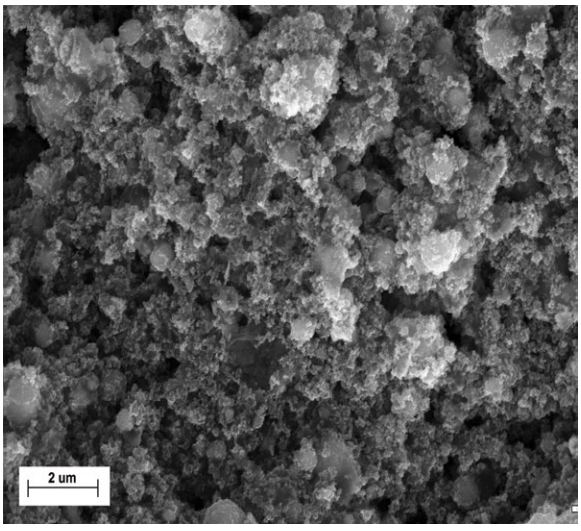


b)

**Figure 1** PSD of: a) $LiNio_2$ and SEM image of: b) $LiNio_2$.

by a mono modal particle size distribution with diameters in the range 825-1720 nm (**Figure 1a**). As evidenced by the SEM image (**Figure 1b**) the particles are regular in shape. The cathode is highly homogeneous, as is confirmed by the low polydispersity index of 0.326. Average particle diameter is lower than for $LiCoO_2$, amounting to 1050 nm.

## Electrolyte liquidity range, viscosity and conductivity

Sulfolan is a five-membered heterocyclic sulfur-organic compound containing a sulfonyl functional group. This group is composed of a sulfur atom connected by double bonds with two oxygen atoms. The sulfur-oxygen double bond is highly polar, ensuring the miscibility of sulfolane with water, while the carbon backbone affects good solubility in hydrocarbons, whereby sulfolane is widely used as a solvent for the purification of hydrocarbon mixtures.

Melting point of sulfolane is relatively high (301.6 K (ca. 28°C)) [40] and hence, it is solid at room temperature. Consequently, melting point of ca. 1 M solutions is lower by ca. 60 K in comparison to that of pure sulfolane (240 K (ca.-33°C)) which is sufficient from the practical point of view. Due to their high boiling point and cryoscopic constant, solutions in sulfolane are characterized by a broad liquidity range (ca. 300 K). Conductivity of the electrolyte at T=298 K is 2.6 mS $cm^{-1}$, with the activation energy of the conduction process, $E_{\sigma}^{a}$ =l8.4 kJ $mol^{-1}$ [41,42]. Viscosity, η, of sulfolane is relatively high and strongly depends on temperature. Sulfolane viscosity, near its melting point is relatively high (ca. 10 cP at 30°C) [40].

## Charging/discharging

**$LiNiO_2$:** Literature sources contain much information on the obtained capacity for the discussed cathode. $LiNiO_2$ exists in two structural modifications, of which only one is electrochemically active [43]. The theoretical capacity of $LiNiO_2$, assuming 1 Li per $NiO_2$ unit may be extracted, is close to that of the $LiCoO_2$ compound, i.e., ~ 275 $mAhg^{-1}$. Again, in a similar fashion to the cobalt system, a significantly lower capacity is obtained in actual test cells. However, the overall reversible specific capacities reported for $LiNiO_2$ are typically 10-30 $mAhg^{-1}$ higher than those of $LiCoO_2$. Fewer cycles have been reported, but good charge retention is generally observed after >100 cycles. The very small particle size was claimed to be advantageous in one report, but unfortunately no electrochemical data were presented. The cycle life size is strongly dependent on the depth of discharge [44], i.e., high cycle numbers are obtained when the capacity is restricted to about 100-120 $mAhg^{-1}$, while only a few cycles are possible at higher capacities. In addition, the $LiNiO_2$ compound appears to be more difficult to synthesize than the corresponding cobalt oxide, in a modification which is able to reversibly insert lithium to any significant extent. In contrast to $LiCoO_2$, which can be prepared by sintering a mixture of almost any Li, Co and $O_2$ sources under proper temperature conditions, the $LiNiO_2$ compound needs to be prepared under strongly oxidizing conditions. Typical examples include e.g., hydroxide mixtures annealed in an $O_2$ atmosphere, hydroxide and nitrate or by the use of $Na_20_2$ and a Ni source, followed by ion exchange with $LiNO_3$ at an elevated temperature.

The structure of $LiNiO_2$ is described in previous text [45-48], while the structure of $Li_2NiO_2$ is also discussed in previous text [46]. The latter paper also discusses lithium insertion in the approximate range 1<x<2 in $LixNiO_2$, which takes place at about 1.8 V versus Li. This is in contrast to lithium insertion in $LiCoO_2$ where no plateau around this voltage is found [46]. The solid state ionic transport properties of $LiNiO_2$ are discussed in previous text [49] while other physical/chemical properties are given in a number of references [50-52]. Performance results, comparable to those of liquid electrolyte systems, were obtained with Li/$LiNiO_2$, Li/$LiMn_2O_4$, C/$LiNiO_2$ and C/$LiCoO_2$ cells [53], using a PAN based hybrid polymer electrolyte (i.e., polymer-liquid-salt combination, [54]) at room temperature. However, a rapid decay of the capacity with cycling was observed in the early experiments with the carbon anode based systems [55-68]. The half-cells was tested for 50 cycles, but **Figures 2-4** present charging/discharging for the first 20 cycles.

**Figures 2-4** show charge-discharge curves and coulombic efficiency of the Li/$LiNiO_2$ half-cell using: 1 M $LiPF_6$ in TMS+10%VC **(Figure 2)** 1 M $LiNTf_2$ in TMS+10%VC **(Figure 3)** and 1 M LiBOB in TMS+10%VC **(Figure 4).**

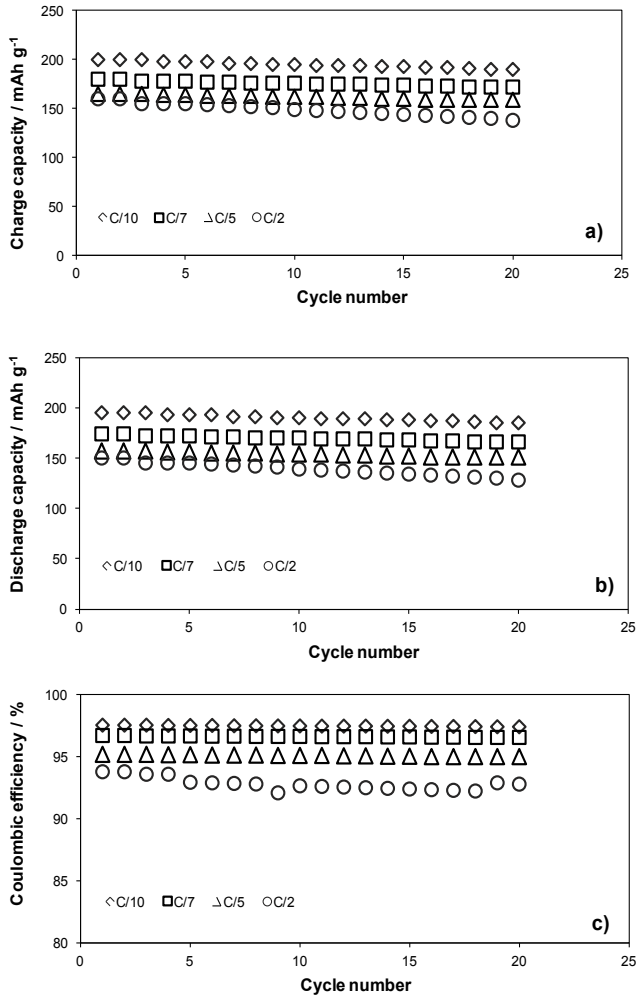


**Figure 2** Charging capacity a) Discharging capacity b) Coulombic efficiency c) of the cell: $LiNiO_2$|1 M $LiPF_6$ in TMS+10%VC |Li (rates: C/10, C/7, C/5, C/2).

The highest capacity is observed for the system Li [1 M $LiPF_6$ in TMS+10%VC] $LiNiO_2$. The capacity of the charging (deintercalation) and discharging (intercalation) processes after 20 cycles was 200 $mAhg^{-1}$ and 195 $mAhg^{-1}$, resulting in a coulombic efficiency of 98% under the current rate C/10. Moreover when the current is increased from C/10 to C/2 charge and discharge capacity decreases after 20 cycles to 144 $mAhg^{-1}$ and 135 $mAhg^{-1}$, respectively **(Figure 2)** the reversible capacity is not low and accounts for 70% of the theoretical value, which is a good result with promising prospects for further research. Slightly worse properties of the $LiNiO_2$ cathode are observed for other electrolytes. The charging/discharging capacity for Li [1 M $LiNTf_2$ in TMS+10%VC] $LiNiO_2$ is found within a range of 180-170 $mAhg^{-1}$ and 170-162 $mAhg^{-1}$ resulting in a coulombic efficiency of 95% (current is increased than charge and discharge capacity decreased) **(Figure 3).**

The lowest coulombic efficiency, of about 90%, is observed for the system Li [1 M LiBOB in TMS+10%VC] $LiNiO_2$. The electrolyte containing LiBOB was the least stable during the charging/discharging process **(Figure 4).**

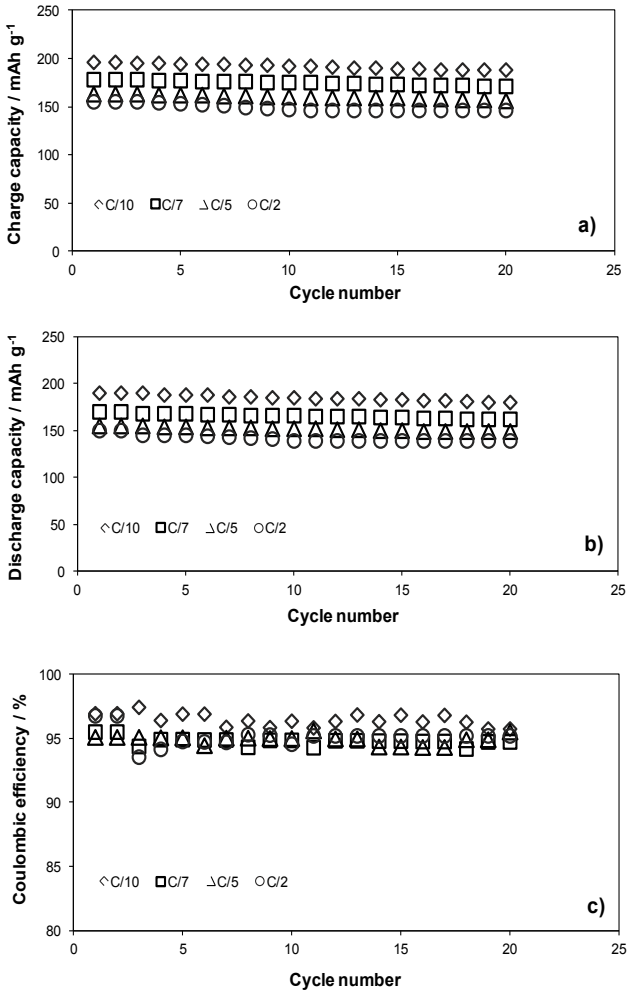


**Figure 3** Charging capacity a) Discharging capacity b) Coulombic efficiency c) of the cell: $LiNiO_2$|1 M $LiNTf_2$ in TMS+10%VC |Li (rates: C/10, C/7, C/5, C/2).

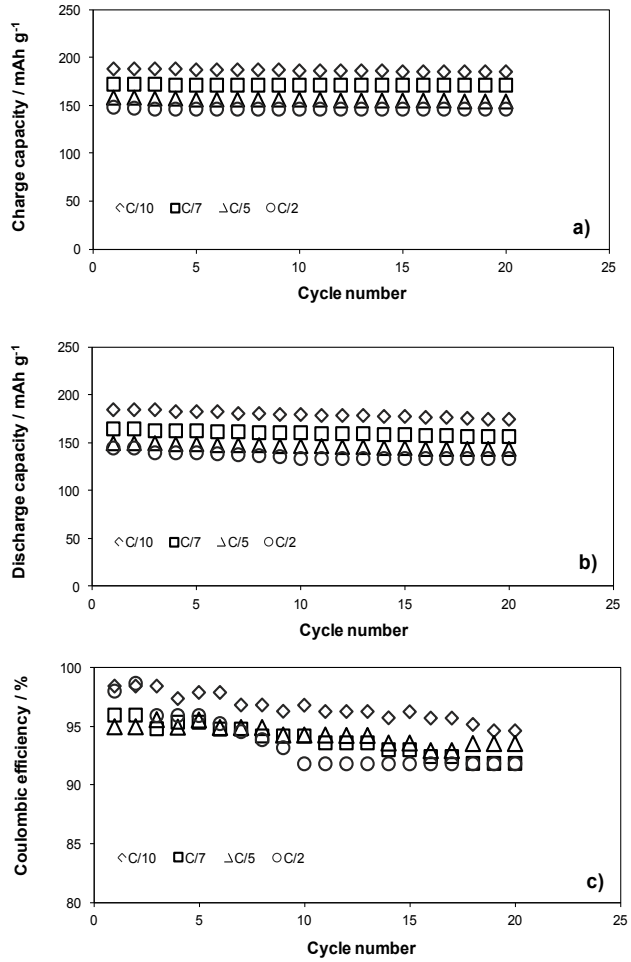


**Figure 4** Charging capacity a) Discharging capacity b) Coulombic efficiency c) of the cell: $LiNiO_2$|1 M LiBOB in TMS+10%VC |Li (rates: C/10, C/7, C/5, C/2).

## Electrolyte flammability

In lithium-ion cells containing classical electrolytes the solvent may start to evaporate and consequently, the vapour may ignite. Therefore, for safety reasons, it is of practical significance to look for new non-volatile electrolytes. Many ionic liquids, due to the strong ion–ion interactions, are characterized by negligible vapour pressure at room temperature. On the other hand, the SEI forming additives, such as VC, are volatile organic compounds and it is necessary to estimate the flash point of such mixtures **(Figure 5).**

Flash points of ethylene carbonate and propylene carbonate are 143°C and 123°C, respectively (Sigma-Aldrich and Merck catalogues), while in the case of dimethyl carbonate it is only 16°C (Sigma-Aldrich catalogue). Flash point of neat sulfolane is much higher than 177°C [40]. In addition, if the electrolyte in cyclic carbonates is in contact with the cathode, the flash point may be reduced. The system under study: i.e., $LiNiO_2$ (solid)+1 M $LiPF_6$+TMS+10%VC have a flash point of ca. 160°C. This is much higher in comparison to that characteristic of a classical $LiNiO_2$(solid)+1 M $LiPF_6$+EC 50%+DMC 50% system ($T_f$=42°C).

During SEI formation the volatile additive (VC) is converted into a solid polymeric component of the interface. Consequently, the amount of the volatile compound decreases to a low value, increasing the flash point of the electrolyte. The flash point determined for the: $LiPF_6$ solution in TMS, without VC, is 168°C, $LiNTf_2$ solution in TMS, without VC, is 155°C and $LiPF_6$ solution in TMS, without VC, is 153°C.

**Figure 6** shows thermal gravimetric analysis (TG/DTA) of the 1 M $LiPF_6$+TMS+10%VC electrolyte under nitrogen atmosphere. It can be seen that the main decomposition peak of the electrolyte (both liquid solvents and the lithium salt) is found at ca.275°C. The TG/DTA profiles shown in **Figure 6** are similar to those found to poly vinylidene fluoride-based gel electrolyte [42].

No significant differences were observed in the TG/DTA for other electrolytes (1 M $LiNTf_2$+TMS+10%VC or 1 M LiBOB+TMS+10%VC). The peak appears at approximately 260°C-280°C (**Figures 7 and 8**).

## Cyclic voltammetry

A cyclic voltammogram of the Pt [1 M $LiPF_6$ in TMS+10%VC] system is given in literature [68]. Cyclic voltammograms of the graphite electrode in 1 M $LiNTf_2$ dissolved in TMS is shown in **Figure 9a** Examination of the curve of the first cycle (the first reduction process) shows two fine peaks around 0.2 and 0.7 V, presumably corresponding to the formation of SEI on the surface anode. These peaks which disappear completely with further cycling are apparently due to VC reductions. The next stage of lithium intercalation occurs at potential below 0.3 V and reaches a peak at a potential 0.005 V. The difference between the CV curve of the first cycle and subsequent cycles indicates that the irreversible capacity mainly occurs in the first cycle. A similar

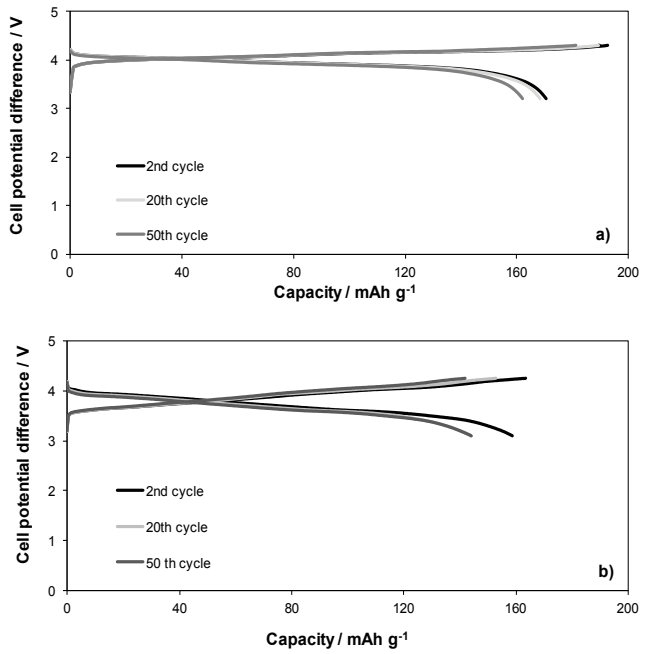


**Figure 5** Galvanostatic charging and discharging of: a) $LiNiO_2$/1 M $LiPF_6$ in TMS+10% wt. VC/Li, b) $LiCoO_2$/1 M $LiPF_6$ in TMS+10% wt. VC /Li system (2nd, 20th, 50th cycles) at C/5 rate.

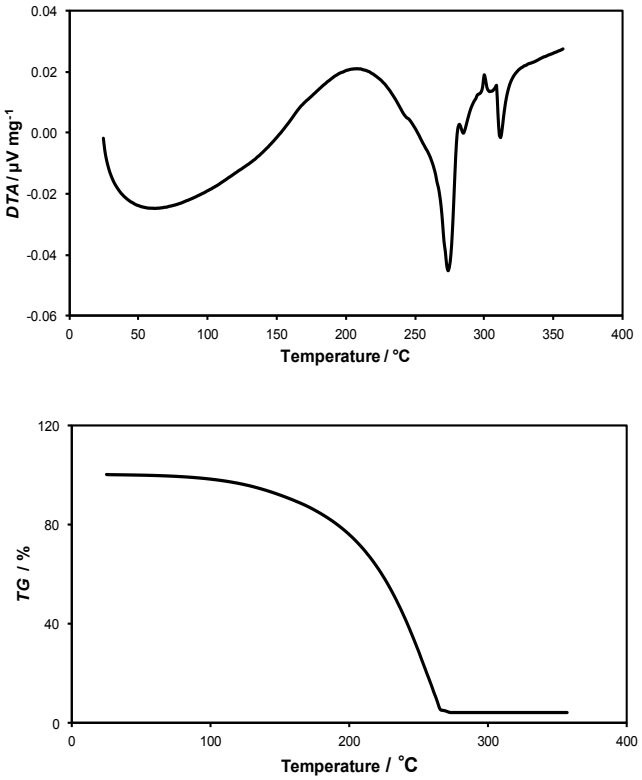


**Figure 6** TG/DTA profiles related to the heating test of the 1 M $LiPF_6$+TMS+10%VC electrolyte under nitrogen atmosphere.

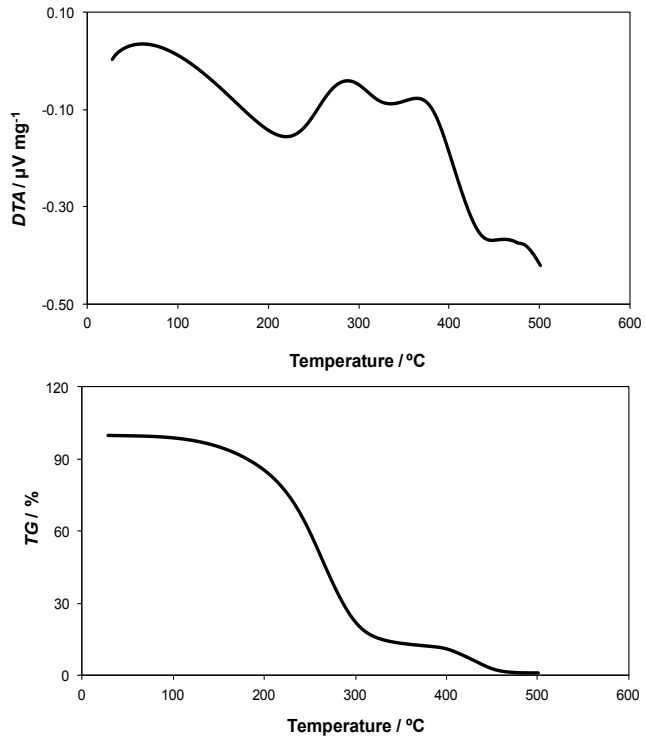


**Figure 7** TG/DTA profiles related to the heating test of the 1 M $LiNTf_2$+TMS+10%VC electrolyte under nitrogen atmosphere.

picture is observed in the case of the second electrolyte, i.e., 1 M LiBOB dissolved in TMS **(Figure 9b).**

## Impedance studies

For a system containing lithium salt: $LiNTf_2$ in TMS was decided to perform a comparative study by performing temperature impedance spectrum. **Figures 10a and 10b** have impedance spectra of $C_6Li|$ $LiNTf_2$ in TMS $|Li$ and $LiNiO_2|LiNTf_2$ in TMS$|Li$ cells. Spectra were deconvoluted according to the equivalent circuit shown in **Figure 10c.** The conductivity of 1.0 M $LiNTf_2$ in TMS at 25°C was 2.6 mS $cm^{-1}$, with the activation energy of the conduction process $E_\sigma^a$ =l8.4 kJ $mol^{-1}$. Therefore, the specific conductivity of the electrolyte at 90°C was 9.8 mS $cm^{-1}$, which is comparable to the corresponding value characteristic of classical solutions in cyclic carbonates working at room temperature. Corresponding resistance of the electrolyte in cells, $R_{el}$, was somewhat higher than that expected from its conductance, due to the porous structure of both electrodes. However, at 90°C it decreased considerably to ca. 8 Ω.

The resistance of the SEI layer, $R_{SEI}$, formed at 25°C on the graphite anode and the $LiNiO_2$ cathode was ca. 9 Ω and 51 Ω, respectively. The corresponding value for SEI formed at 90°C, was higher, achieving 32 Ω ($C_6Li$) and 67 Ω ($LiNiO_2$). A possible explanation is that at a higher temperature the thickness of the formed SEI layer was higher.

The corresponding charge transfer resistance for the $LiNiO_2|Li^+$ cathode (ca. 2.80 mg, BET specific area 15.4 $m^2$ $g^{-1}$, real surface area A=431 $cm^2$) was lower: ca. 5.96 × $10^{-5}$ A $cm^{-2}$ and 7.26 × $10^{-5}$ A $cm^{-2}$ at 25°C and 90°C, respectively.

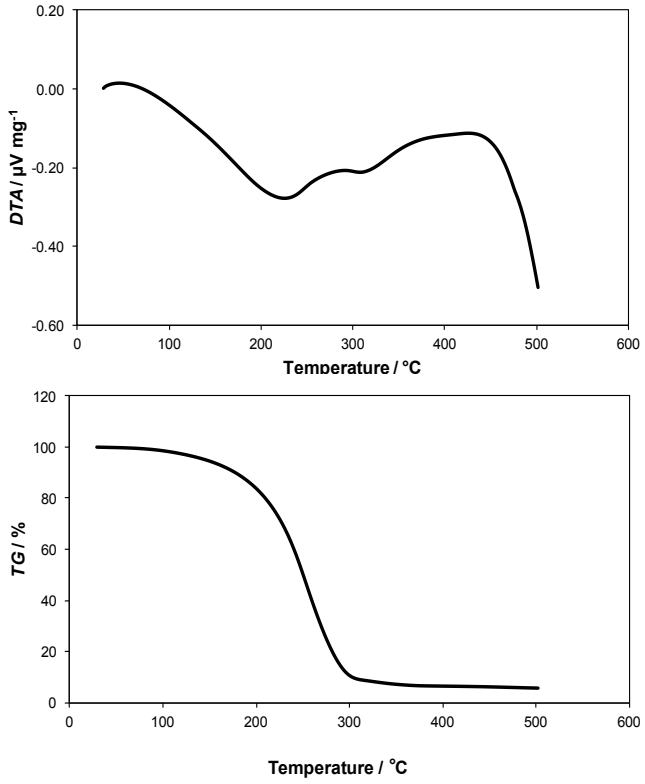


**Figure 8** TG/DTA profiles related to the heating test of the 1 M LiBOB+TMS+10%VC electrolyte under nitrogen atmosphere.

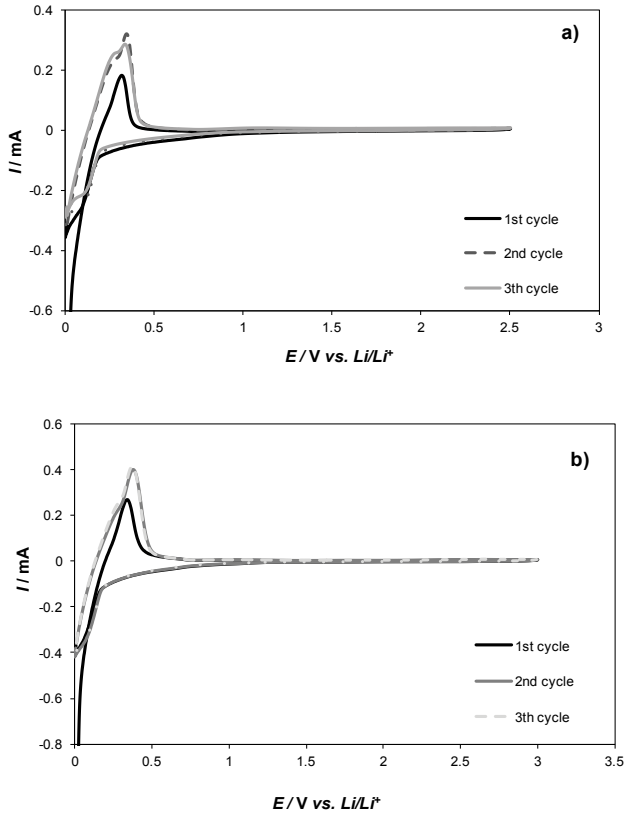


**Figure 9** Cyclic voltammogram of graphite with: a) 1 M $LiNTf_2$ in TMS+10%VC and b) 1 M LiBOB in TMS+10%VC vs. $Li/Li^+$.

The line at the low-frequency region is due to the diffusion of the electro-active species. Generally, any software system used for EIS curve deconvolution applies the Warburg model, which is based on a symmetrical constant phase element. Hence, the diffusion process was approximated here also by the Warburg element $Z_W$. Slopes of linear parts of impedance spectra were not exactly 45°C as predicted by the Warburg model. Moreover, in the case of the $C_6Li|Li^+$ anode, the diffusion impedance increases with an increasing temperature which is difficult to explain. However, the $LiNiO_2$ cathode diffusion impedance decreases considerably with the temperature increase. Numerical evaluation of the diffusion coefficient of Li in the graphite anode or the $LiNiO_2$ cathode is impossible as the concentrations of diffusing species in the solid state have been unknown.

# Conclusion

The solvent used to lower flammability - sulfolane, has a high melting point of 27.5°C. Sulfolane would greatly limit the range of temperatures where it can be used. For these reason we need to add lithium salts, which modify mixture facilitating better use in li-ion batteries. The study tested the addition of salts ($LiPF_6$, $LiNTf_2$ and LiBOB) to sulfolane and efficiency for each cell cathodes ($LiNiO_2$ and $LiCoO_2$).

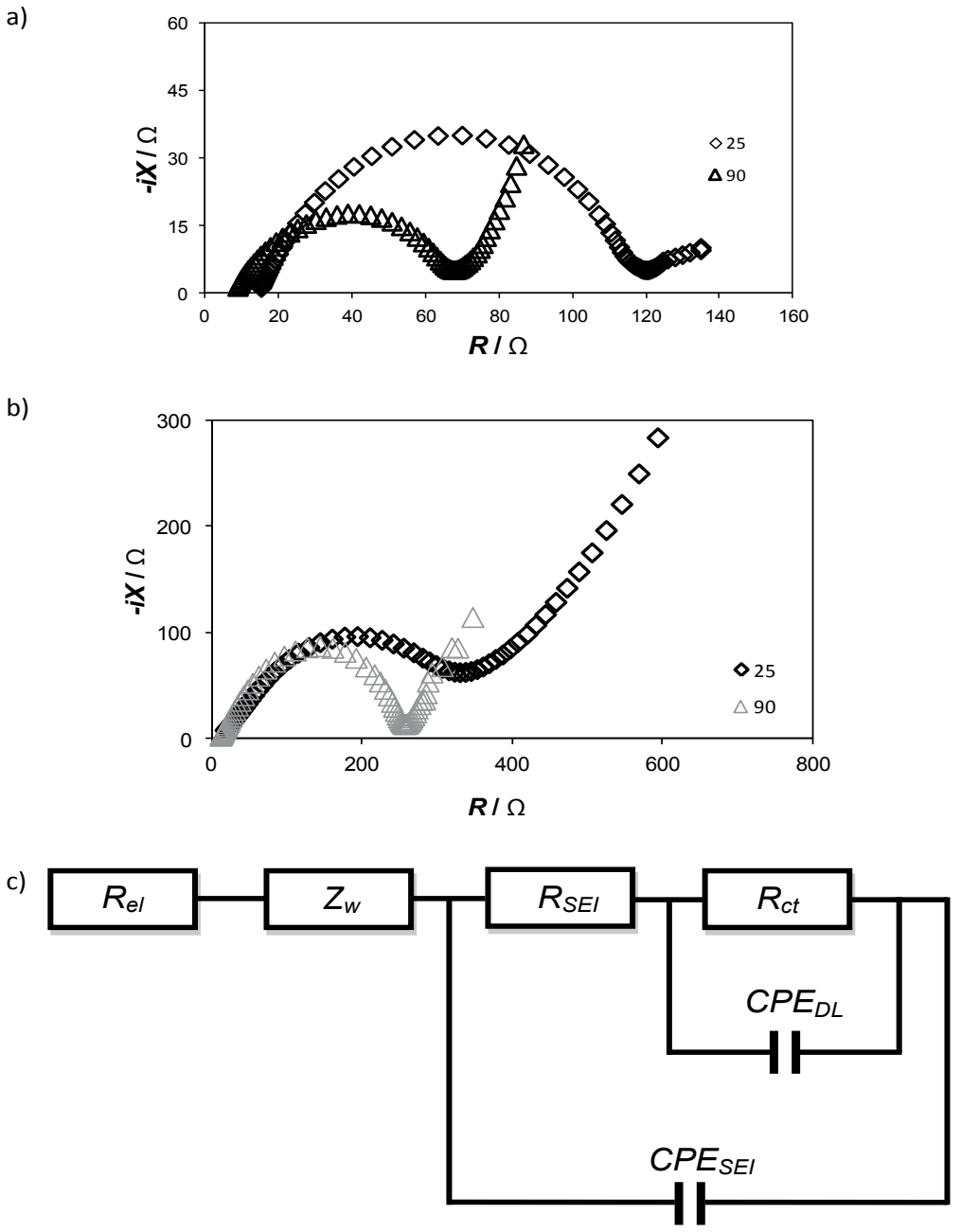


**Figure 10** Impedance spectra of $C_6Li|Li$ system is a function of temperature. Lithiated graphite electrode ($C_6Li$). Graphite mass: 3.49 mg (a), Impedance spectra of the $LiFePO_4|Li$ system as a function of temperature. $LiNiO_2$ mass: 2.80 mg (b) electrodes were after three working cycles (intercalation de intercalation/intercalation). Equivalent circuit used for impedance spectra deconvolution of the $LiNiO_2|SEI|Li^+$ and $LiC_6|SEI|Li^+$ systems (c).

1. These results show that sulfolane with an addition of $LiPF_6$, $LiNTf_2$ and LIBOB can be a good electrolyte for application in Li-ion batteries using cathode: $LiNiO_2$ Charging/discharging capacity was stable and occurs between 200-180 $mAhg^{-1}$ for $LiNiO_2|Li$ system. The value depends on the current rate. Coulombic efficiency was 90-95%.
2. Moreover these electrolytes: 1 M $LiPF_6$ in TMS+10%VC; 1 M $LiNTf_2$ in TMS+10%VC and 1 M LiBOB in TMS+10%VC have good cathodic stability and flash points above 160°C.
3. It can be seen from the thermal gravimetric analysis (TG/DTA) of the electrolytes under nitrogen atmosphere that the main decomposition peak of the electrolyte (both liquid solvents and the lithium salt) is present at ca. 275°C.

## Acknowledgements

Support of grant 03/31/DSPB/0355 is gratefully acknowledged.

## References


1 Kyerematenga NA, Dumur F, Knauth P, Pecquenard B, Djenizian T, et al. (2011) Electro polymerization of copolymer electrolyte into titania nanotube electrodes for high-performance 3D micro batteries. Electrochem Commun 13: 894-897.

2 Oudenhoven JFM, Baggetto L, Notten PHL (2011) All-Solid-state lithium-ion Micro batteries. Review of various three-dimensional concepts. Adv Energy Mater 1: 10-33.

3 Jeevan Kumar P, Jayanth Babu K, Hussain OM (2012) RF Magnetron Sputter Deposited Nanocrystalline $LiCoO_2$ Film Cathodes on Flexible Substrates. Adv Sci Eng Med 4: 190-199.

4 Jayanth Babu K, Jeevan Kumar P, Hussain OM, Julien CM (2012) Influence of annealing temperature on microstructural and electrochemical properties of rf-sputtered $LiMn_2O_4$ film cathodes. J Solid State Electrochem 16: 3383-3390.

5 Stockhoff T, Gallasch T, Berkemeier F, Schmitz G (2012) Ion beam sputter-deposition of $LiCoO_2$ films. Thin Solid Films 520: 3680-3674.

6 Manthiram A, Choi J, Choi W (2006) Factors limiting the electrochemical performance of oxide cathodes. Solid State Ionics 177: 2629-2634.

7 Tintignac S, Baddour-Hadjean R, Pereira-Ramos JP, Salot R (2014) Electrochemical properties of high rate bias sputtered $LiCoO_2$ thin films in liquid electrolyte. J Power Sources 245: 76-82.

8 Park HY, Nam SC, Lim YC, Choi KG, Lee KC, et al. (2007) Electrochim Acta 52: 2062-2067

9 Chen ZZ, Shi EW, Li WJ, Zheng YQ, Zhuang JY, et al. (2004) Preparation of nano sized cobalt aluminate powders by a hydrothermal method. Mater Sci Eng B 107: 217-223.

10 Fujimoto K, Ikezawa K, Ito S (2011) Charge-discharge properties of a layered-type Li (Ni, Co, Ti)$O_2$ powder library. Sci Technol Adv Mater 12: 054203-054206.

11 Rao MC, Hussain (2010) Synthesis and electrochemical properties of Ti doped $LiCoO_2$ thin film cathodes. J Alloys Compd 491: 503-506.

12 Lu YC, Mansour AN, Yabuuchi N, Horn YS (2009) Probing the origin of enhanced stability of $AlPO_4$ nanoparticle coated $LiCoO_2$ during cycling to high voltages. Combined XRD and XPS studies. Chem Mater 21: 4408-4424.

13 Gu Y, Chen D, Jiao X (2005) Synthesis and electrochemical properties of nanostructured $LiCoO_2$ fibers as cathode materials for lithium-ion batteries. J Phys Chem B 109: 17901-17906.

14 Okubo M, Hosono E, Kim J, Enomoto M, Kojima N, et al. (2007) Nano size effect on high-rate Li-ion intercalation In $LiCoO_2$ electrode. J Am Chem Soc 129: 7444-7452.

15 Chen H, Wu L, Zhang L, Zhu Y, Grey CP, et al. (2011) $LiCoO_2$ Concaved cuboctahedrons from symmetry-controlled topological reactions. J Am Chem Soc 133: 262-270.

16 Boyle TJ, Rodriguez MA, Ingersoll D, Headley TJ, Bunge SD, et al. (2003) Synthesis and characterization of a novel family of lithium cobalt double alkoxides and the characterization of the nanoparticle and thin films generated there from. Chem Mater 15: 3903-3912.

17 Kramer D, Ceder G (2009) Tailoring the Morphology of $LiCoO_2$. First Principles Study. Chem Mater 21: 3799-3809.

18 Okubo M, Kim J, Kudo T, Zhou H, Honma I, et al. (2009) anisotropic surface effect on electronic structures and electrochemical properties of $LiCoO_2$. J Phys Chem C 113: 15337-15342.

19 Dahn R, Sacken U, Juzkow MW, Al-Janaby H (1991) Rechargeable $LiNiO_2$/carbon cells. J Electrochem Soc 138: 2207-2211.

20 Ebner W, Fouchard D, Xie L (1994) The LiNiOZ/carbon lithium-ion battery. Solid State Ionics 69: 238-256.

21 Mizushima K, Jones PC, Wiseman PC, Goodenough JB (1980) $LixCoO_2$ (0<x ≤ l) a new cathode material for batteries of high energy density. Mater Res Bull 15: 783-789.

22 Ozawa K (1994) Lithium-ion rechargeable batteries with $LiCoO_2$ and carbon electrodes: the $LiCoO_2$/C system. Solid State Ionics 69: 212-221.

23 Nithya C, Thirunakaran R, Sivashanmugam A, Gopukumar S (2012) High-Performing $LiMg_xCu_yCo_{1-x-y}O_2$ Cathode Material for Lithium Rechargeable Batteries. Appl Mater Interf 4: 4040-4046.

24 Myung, Kumagai N, Komaba S, Chung (2000) Preparation and electrochemical characterization of $LiCoO_2$ by the emulsion drying method. J Appl Electrochem 30: 1081-1085.

25 Kumta PN, Gallet D, Waghray A, Blomgren GE, Setter MP, et al. (1998) Synthesis of $LiCoO_2$ powders for lithium-ion batteries from precursors derived by rotary evaporation. J Power Sources 72: 91-98.

26 Seung-Taek M, Shinichi K, Naoaki K (2002) Hydrothermal synthesis of orthorhombic $LiCoxMn_1$-$xO_2$ and their structural changes during cycling. J Electrochem Soc 149: A1349-A1357.

27 Imanishi N, Fujii M, Hirano A, Takeda Y, Inaba M, et al. (2001) Structure and electrochemical behaviors of $Li_xCoO_2$ (x>l) treated under high oxygen pressure. Solid State Ionics 140: 45-53.

28 Kannan AM, Rabenberg L, Manthiram A (2003) High capacity surface-modified $LiCoO_2$ cathodes for lithium-ion batteries. Electrochem Solid-State Lett 6: A16-A18.

29 Chen HL, Wu LJ, Zhang LH, Zhu YM, Grey CP, et al. (2011) $LiCoO_2$ Concaved cuboctahedrons from symmetry-controlled topological reactions. J Am Chem Soc 133: 262-270.

30 Arroyo y de Dompablo ME, Ceder G (2003) First-principles calculations on $Li_xNiO_2$. Phase stability and monoclinic distortion. J Power Sources 119-121: 654-657.

31 Ohzuku T, Ueda A, Nagayama M (1993) Electrochemistry and structural chemistry of $LiNiO_2$ (R3m) for 4 volt secondary lithium cells. J Electrochem Soc 140: 1862-1870.

32 Chowdari BVR, Subba Rao GV, Chow SY (2001) Cathodic Behavior. Solid State Ionics 140: 55-62.

33 Park SH, Park KS, Sun Kook Y, Nahm KS, Lee YS, et al. (2001) Structural and electrochemical characterization of lithium excess and Al-doped nickel oxides synthesized by the sol-gel method. Electrochim Acta 46: 1215-1222.

34 Makimura Y, Ohzuku T (2003) Lithium insertion material of $LiNi_{1/2}Mn_{1/2}O_2$ for advanced Li-ion battery. J Power Sources 119-121: 156-160.

35 Nishida Y, Nakane K, Satoh T (1997) Synthesis and properties of gallium-doped $LiNiO_2$ as the cathode material for lithium secondary batteries. J Power Sources 68: 561-564.

36 Chiu CC, Li CC, Desu SB (1991) Molten salt synthesis of a complex perovskite $Pb(Fe_{0.5}Nb_{0.5})O_3$. J Am Ceram Soc 74: 38-41.

37 Yoon KH, Cho YS, Lee DH, Kang DH (1993) Powder characteristics of $Pb(Mg_{1/3}Nb_{2/3})O_3$ prepared by molten salt synthesis. J Am Ceram Soc 76: 1373-1376.

38 Han CH, Hong YS, Park C, Kim K (2001) Synthesis and electrochemical properties of lithium cobalt oxides prepared by molten-salt synthesis using the eutectic mixture of LiCl-$Li_2CO_3$. J Power Sources 92: 95-101.

39 Han CH, Hong YS, Kim K (2003) Cyclic performances of HT-$LiCo_{0.8}M_{0.2}O_2$ (M=Al, Ni) powders prepared by the molten salt synthesis method. Solid State Ionics 159: 241-247.

40 Martinmaa J, Lagowski JJ (1976) Sulfolane in the Chemistry of Nonaqueous Solvents. Academic Press, New York.

41 Kolosnitsyn VS, Sheina LV, Mochalov SE (2008) Physicochemical and electrochemical properties of sulfolane solutions of lithium salts. Russ J Electrochem 44: 575-578.

42 Hassoun J, Reale P, Panero S, Scrosati B, Wachtler M, et al. (2010) Determination of the safety level of an advanced lithium ion battery having a nanostructured Sn-C anode, a high voltage $LiNi_{0.5}Mn_{1.5}O_4$ cathode, and a polyvinylidene fluoride-based gel electrolyte. Electrochim Acta 55: 4194-4200.

43 Ohzuku T, Ueda A, Nagayama M, Iwakoshi Y, Komori H (1993) Comparative study of $LiCoO_2$, $LiNi_{12}Co_{12}O_2$ and $LiNiO_2$ for 4 volt secondary lithium cells. Electrochimic Acta 38: 1159-1167.

44 Yamada S, Fujiwara M, Kanda M (1995) Synthesis and properties of $LiNiO_2$ as cathode material for secondary batteries. J Power Sources 54: 209-213.

45 Wells AF (1984) Structural Inorganic Chemistry. Oxford Science Publications (Clarendon Press), p: 577.

46 Dahn JR, von Sacken U, Michal CA (1990) Structure and electrochemistry of $Li_{1\pm y}NiO_2$ and a new $Li_2NiO_2$ phase with the Ni $(OH)_2$ structure. Solid State Ionics 44: 87-92.

47 Li W, Reimers JN, Dahn JR (1994) Lattice-gas-model approach to understanding the structures of lithium transition-metal oxides $LiMO_2$. Phys Rev B 49: 826-831.

48 Hirano A, Kanno R, Kawamoto Y, Takeda Y, Yamaura K, et al. (1995) Relationship between non-stoichiometry and physical properties in $LiNiO_2$. Solid State Ionics 78: 123-131.

49 Bruce PG, Lisowska-Oleksiak A, Saidi MY, Vincent CA (1992) Vacancy diffusion in the intercalation electrode $Li_1xNiO_2$. Solid State Ionics 57: 353-360.

50 Reimers JN, Dahn JR, Greedan JE, Stager CV, Liu G, et al. (1993) Spin Glass Behavior in the Frustrated Antiferromagnetic $LiNiO_2$. J Solid State Chem 102: 542-552.

51 Hirakawa K, Kadowaki H (1986) The ground states and phase transitions in the two-dimensional triangular lattice anti Ferro magnets. Physica B+C 136: 335-340.

52 Good Enough JB, Wickham DG, Croft WJ (1958) Some Ferromagnetic Properties of the System $Li_xNi_{1-x}O$. J Appl Phys 29: 382-383.

53 Abraham KM, Alamgir M (1993) Ambient temperature rechargeable polymer-electrolyte batteries. J Power Sources 43-44: 195-208.

54 Koksbang R, Olsen II, Shackle D (1994) Review of hybrid polymer electrolytes and rechargeable lithium batteries. Solid State Ionics 69: 320-335.

55 Mizushima K, Jones PC, Wiseman PJ, Goodehough JB (1980) $Li_xCoO_2$ (0<x<-1) A new cathode material for batteries of high energy density. Mater Res Bull 17: 783-799.

56 Delmas C (1989) Alkali metal intercalation in layered oxides. Mater Sci Eng B 3: 97-101.

57 Reimers JN, Rossen E, Jones CD, Dahn JR (1993) Structure and electrochemistry of $Li_xFe_yNi_{1-y}O_2$. Solid State Ionics 61: 335-344.

58 Wells AF (1984) Structural Inorganic Chemistry. 5th edn. Oxford Science Publications, pp: 577-582.

59 Gao Y, Myrtle K, Zhang M, Reimers JN, Dahn JR (1996) Valence band of $LiNi_xMn_{2-x}O_4$ and its effects on the voltage profiles of $LiNi_xMn_{2-x}O_4$/Li electrochemical cells. Phys Rev B Condens Matter 54: 16670-16675.

60 Gummow RJ, Liles D, Thackeray M (1993) Lithium extraction from orthorhombic lithium manganese oxide and the phase transformation to spinel. Mater Res Bull 28: 1249-1256.

61 Reimers JN, Dahn JR (1992) Electrochemical and in situ X-ray diffraction studies of lithium intercalation in $Li_xCoO_2$. J Electrochem Soc 139: 2091-2097.

62 Gummow R, Thackeray MM (1993) Characterization of LT-Li(x)Co(1-y) Ni(y)$O_2$ electrodes for rechargeable lithium cells. J Electrochem Soc 140: 3365-3368.

63 Thomas MGSR, Bruce PG, Goodenough JB (1985) Lithium mobility in the layered oxide $Li_1xCoO_2$. Solid State Ionics 17: 13-19.

64 Ma Y, Doeff Marca M, Visco Steven J, De Jonghe Lutgard C (1993) Rechargeable Na/$NaxCoO_2$ and $Na_{15}Pb_4$/$NaxCoO_2$ polymer electrolyte cells. J Electrochem Soc 140: 2726-2733.

65 Thomas MGSR, Bruce PG, Goodenough JB (1985) AC impedance analysis of polycrystalline insertion electrodes. Application b Li//1// minus//xCoO//2. J Electrochem Soc 132: 1521-1528.

66 Peled E, Gabano JP (1983) Education in Lithium Batteries. Academic Press, London, UK, pp: 43-72.

67 Koksbang R, Barker J, Shi H, Saidi MY (1996) Cathode materials for lithium rocking chair batteries**.** Solid State Ionic 84: 1-21.

68 Lewandowski A, Kurc B, Stepniak I, Swiderska-Mocek A (2011) Properties of Li-graphite and $LiFePO_4$ electrodes in $LiPF_6$ sulfolane electrolyte. Electrochim Acta 56: 5972-5978.